Correlation between crystallographic texture and the degree of $L1_0$-ordering in post-annealed Ag/CoPt bilayers and comparison with Ag/CoPt nanocomposites

Journal of Physics: Conference Series **153** (2009) 012060 doi:10.1088/1742-6596/153/1/012060

Correlation between crystallographic texture and the degree of $L1_0$-ordering in post-annealed Ag/CoPt bilayers and comparison with Ag/CoPt nanocomposites

E Manios[1], D Stamopoulos[1], I Panagiotopoulos[2] and D Niarchos[1]

[1] Institute of Materials Science, NCSR "Demokritos", 153-10, Aghia Paraskevi, Athens, Greece
[2] Department of Materials Science and Engineering, University of Ioannina, 451-10, Ioannina, Greece

E-mail: manios@ims.demokritos.gr (E Manios)

Abstract. CoPt and FePt compound films with $L1_0$ ordered structure have been intensively studied, due to their extremely high uniaxial magnetocrystalline anisotropy which makes them suitable for application in ultra high density magnetic recording media. A basic requirement in these type of media is the development of strong perpendicular magnetic anisotropy. The role of Ag underlayers in promoting strong (001) crystallographic texture and perpendicular magnetic anisotropy in post-annealed Ag/CoPt and Ag/FePt bilayers (BLs) has already been reported, along with a possible correlation between $L1_0$ formation and development of (001) crystallographic texture. In this work we present new data, which provide further evidence that there is indeed such a correlation during the annealing process of Ag/CoPt BLs. The most obvious manifestation of this correlation is the fact that the X-ray intensity ratios I_{001}/I_{002} (used as a measure of the degree of $L1_0$-ordering) and I_{002}/I_{111} (used as a measure of the crystallographic texture) and the coercivity H_c and relative remnant magnetization m_r (for field H normal to the surface of the films) exhibit the same kind of dependence from the thickness of the Ag underlayer. Comparison with respective crystallographic data from post-annealed Ag/CoPt nanocomposites (NCs) shows that in the case of NCs the (001) texture starts to degrade for lower total film thickness, compared to the case of BLs. This difference can be attributed to the structural incoherence in the growth of the CoPt grains imposed by the presence of Ag inside the Ag/CoPt NCs, while in BLs Ag is only used as an underlayer. Based on the above data and on detailed Heavy Ion Elastic Rutherford Back Scattering (HIRBS) measurements, performed on post-annealed Ag/CoPt NCs, we propose a possible mechanism for the interpretation of the observed correlation. The proposed mechanism is based on the reduction of total strain (residual strain of as-deposited film and transformation strain due to deformation of the unit cell as $L1_0$-CoPt is formed) throughout the annealing process.

1. Introduction

Co-Pt and Fe-Pt alloys with almost equiatomic stoichiometry (CoPt and FePt) have been studied in the past, for use as permanent magnets. CoPt and FePt are disordered single-phase solid solutions with FCC crystal structure above 820^{o}C for CoPt and above 1300^{o}C for FePt. *Below these critical temperatures they undergo a long-range ordering phase transformation* [1, 2, 3, 4] *to a structure known as the CuAu-I type* [3, 4, 5] *or face centered tetragonal (FCT) or* $L1_0$. The

unit cell of this structure is tetragonal, with the (002) planes (normal to the [001]-axis or c-axis with distance $c/2$ between successive planes) occupied alternately by Co and Pt atoms for CoPt or by Fe and Pt atoms for FePt [1, 2, 5] and the c-axis smaller than a and b axes. The $L1_0$ phase of both CoPt and FePt is characterized by large uniaxial (along c-axis) magnetocrystalline anisotropy, with reported bulk values $K_u \sim 5\times10^7$ erg/cm^3 for CoPt and $K_u \sim 7\times10^7$ erg/cm^3 for FePt [6, 7, 8, 9, 10, 11, 12, 13]. This high anisotropy constant K_u is the reason why $L1_0$ structured CoPt and FePt are possible candidates for use in high density magnetic recording media [14, 15, 16, 17, 18, 19, 20], in the form of thin films [14, 21, 22, 23, 24, 25, 26, 27, 28] and nanocomposite thin films [25, 29, 30, 31, 32, 33, 34, 35, 36]. The reported K_u values for CoPt and FePt are at least 20 times higher than these of the currently used Co-alloy based media, like CoPtCr [17]. The minimum size D_p, for which the energy of exchange coupling between the spins is sufficiently larger than thermal energy and is able to maintain the ferromagnetic state of the particle/grain (superparamagnetic limit), is estimated to be approximately $D_p=(60kT/K_u)^{1/3}$ [16, 17]. This gives a critical particle size well below 10 nm: it is $D_p \sim 3$–4 nm for CoPt and FePt at room temperature [16, 17]. Due to this values of D_p for CoPt and FePt, it is expected that we can use at least 3 times smaller particle diameters D [17]. The result is a potential 10-fold areal density increase, since the areal density is analogous to $1/D^2$ [17]. Therefore the size of the CoPt or FePt grains can be reduced significantly without affecting the thermal stability of the recording medium.

Additional requirements (along with high K_u) that must be satisfied by a thin film with CoPt or FePt, in order to be suitable for use in magnetic recording, are:

(a) Grain isolation for reduction of the noise caused by inter-grain interactions and further increment the thermal stability.

(b) High coercivity H_c, which assures that small fields can not reverse the magnetization of grains. Coercivity is connected to uniaxial anisotropy, and therefore this requirement is not independent from the basic requirement for high anisotropy.

(c) Narrow width of grain size distribution, because in this case the width of the distribution of magnetic fields – that are needed for magnetization reversal in the grains – is also narrow (around H_c). The narrow width in the distribution of magnetic fields results in square-shaped hysteresis loops. This assures that the grain magnetization will not be affected from a field opposite to it, if the strength of this field is smaller than coercivity H_c.

(d) Crystallographic texture, since in this case the easy axis of magnetization of each grain is highly aligned towards a specific direction and produce a square-shaped loop in this direction. The most interesting case is the development of (001) texture, where the direction of alignment of the easy axis is normal to the plane of the film. This arrangement is magnetostatically favorable, since it reduces the magnetostatic interaction between successive bit cells, and allows the significant increment of the areal density of stored bits [37].

In this work we focus our attention on the development of (001) crystallographic texture. It has been reported that this kind of texture can be the result of suitable deposition and/or annealing conditions, which may be combined with the use of specific additives such as Ag, C, B_2O_3, SiO_2, BN and B_4C [23, 25, 27, 28, 30, 33, 34, 38, 39, 40, 41, 42, 43, 44, 45, 46, 47, 48, 49, 50]. In particular, it has been reported that the use of Ag underlayers [27, 28] is a very effective method for the development of strong (001) texture on CoPt or FePt films. In Ref. [25] we have reported on the influence of thin (of the order of 1.2–1.8 nm) Ag underlayers on the structural and magnetic properties of post-annealed Ag/CoPt BLs. The results of the X-ray measurements presented there, implied that there is a correlation between the degree of FCT-ordering and the degree of (001) crystallographic texture. Here we present additional X-ray data, which are combined with magnetization data. These combined crystallographic and magnetization measurements provide further evidence for the existence of this correlation. Based on these detailed data and on additional Heavy Ion Elastic Rutherford Back Scattering (HIRBS)

measurements, performed on post-annealed Ag/CoPt NCs, we propose a possible interpretation for this correlation. The basic idea of the proposed mechanism is that the development of (001) texture results from the minimization of the elastic energy related to strain. Finally we present comparative data concerning the degree of (001) texture exhibited by BLs and NCs. These data clearly show that, while for small total film thickness (in the range of 9–12 nm) the NCs exhibit a higher degree of (001) texture compared to the BLs, for thicker films the degree of (001) texture of NCs reduces more sharply with the total film thickness. This difference is probably a result of the residual Ag in the interior of the NC films after the annealing process.

2. Preparation of samples and Experimental details

Below we briefly present information on the preparation of the samples used in this work. All the samples were initially deposited by magnetron sputtering on Si(001) substrates at ambient temperature, under an ultra pure Ar environment (99.999%), at a pressure of 3 mTorr. The as-deposited samples were magnetically soft, containing only the disordered FCC phase of CoPt. The base pressure (before inserting Ar) in the sputtering chamber was BP=5×10^{-7} Torr. In order to achieve the transformation from the disordered FCC phase to the highly anisotropic and magnetically hard $L1_0$ phase of CoPt, the films were annealed in high vacuum (10^{-6} Torr). High purity (99.99%) Ag and Co targets (with 2 in diameter) were used for the deposition of the various layers. In the case of the CoPt layers, the Co target was partially covered with Pt. X-ray Fluorescence (XRF) measurements were performed (not shown here), to verify that the atomic stoichiometry of the CoPt layers was close to 50% Co – 50% Pt. For the preparation of the BLs, the Ag and CoPt layers were sequentially deposited on the Si(001) substrates. The Ag layers were deposited by dc-sputtering at 5 W and at a rate of 1.5 Å/sec [25]. The CoPt layers were deposited by rf-sputtering at 30 W and at a rate of 1.2 Å/sec [25]. The as-deposited BLs were annealed for 20 min at 600^oC [25], in order to produce post-annealed BLs with adequate magnetic properties. For annealing at lower temperatures or for shorter time periods, the maximum values of coercivity or relative remnant magnetization – exhibited by the produced BLs – were not satisfying. For the preparation of the NCs, the films were initially deposited in multilayer form and subsequently post-annealed at 600^oC.

X-ray diffraction (XRD) spectra were collected with a SIEMENS D500 powder diffractometer using Cu-Ka radiation. The XRD intensity ratio I_{001}/I_{002} was used as a measure of the degree of $L1_0$-ordering of CoPt. The XRD intensity ratio I_{002}/I_{111} was used as a measure of the crystallographic texture of CoPt. We note here that it is I_{001}/I_{002}=1.286 and I_{002}/I_{111}=0.28 for single-phased, polycrystalline, bulk $L1_0$-CoPt with randomly oriented grains [51]. Comparison of the I_{001}/I_{002} and I_{002}/I_{111} ratios of the samples with these values serves as a measure of $L1_0$-ordering and texture respectively. Magnetic hysteresis loops were obtained at room temperatute with a Digital Measuring System 660 Magneto-Optical Kerr Effect (MOKE) Magnetometer for field H normal ($H\perp$film) and papallel ($H\|$film) to the plane of the films. For $H\|$film, the noise in MOKE magnetic measurements was comparable to the signal. Therefore the results of MOKE measurements for $H\|$film will not be presented. The maximum field that can be produced by the electromagnet of the magnetometer is: H_{max}^{MOKE}=1.2 Tesla. The MOKE hysteresis loops that are presented are normalized (magnetization $M(H)$ divided by the maximum magnetization M_{max}). The coercivity H_c, saturation magnetization M_s, remnant magnetization M_r and relative remnant magnetization m_r=M_r/M_s were determined by performing calculations on the curves that were obtained from fitting equations of the form $M(H,z) = M_0 + M_{S1}\tanh[(H-H_0+zH_{C1})/W_1] + M_{S2}\tanh[(H-H_0+zH_{C2})/W_2]$ with z=±1 in the experimental hysteresis loops M/M_{max}=f(H) with the least squares method. The atomic stoichiometry of Ag/CoPt films, as function of depth, was determined by Heavy Ion Elastic Rutherford Back Scattering (HIRBS) measurements on selected samples. A 8 MeV $^{12}C^{+++}$ beam was used, with surface barrier Si-detector at 170^o with respect to the beam direction,

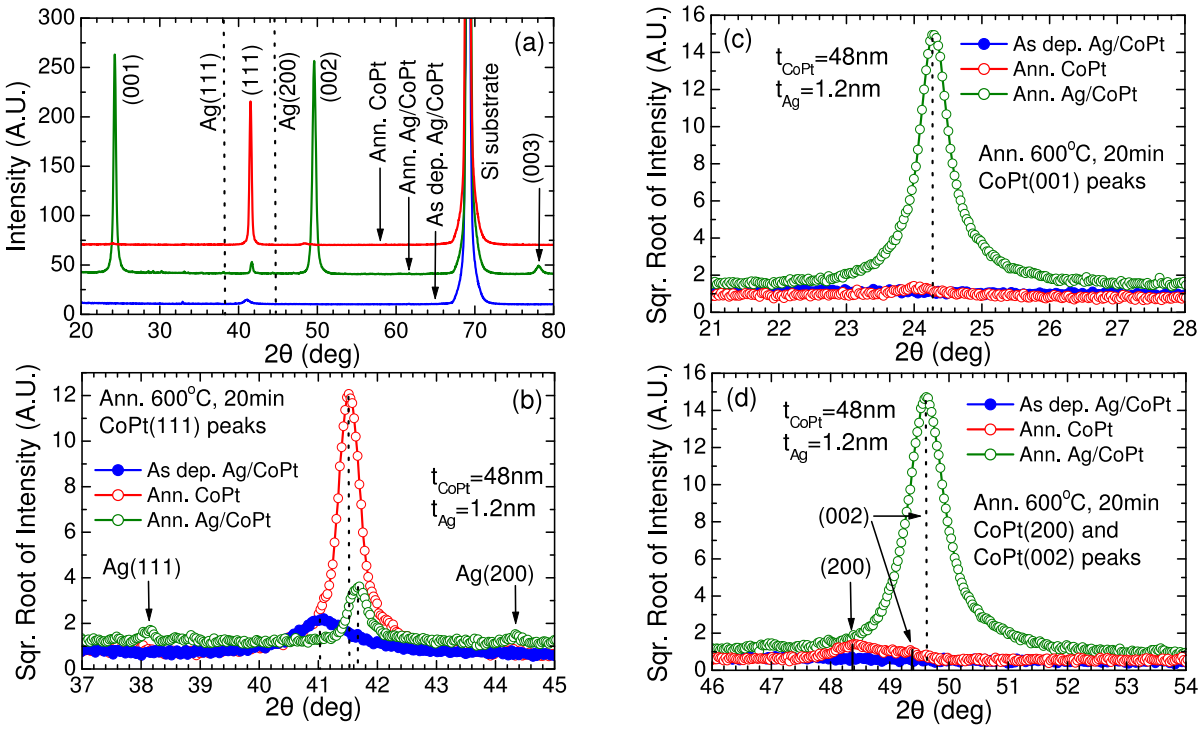

Figure 1. XRD spectra (panel (a)) of a Si(001)/Ag(1.2nm)/CoPt(48nm) BL, as-deposited (bottom) and annealed at 600^{o}C for 20 min (middle). These spectra of the BL are compared to the XRD spectrum of a Si(001)/CoPt(48nm) MNL, annealed at 600^{o}C for 20 min (top). The vertical dotted lines indicate the positions where the two strongest peaks of Ag are expected: $2\theta \approx 38.15^o$ for Ag(111) peak and $2\theta \approx 44.32^o$ for Ag(200) peak. Panels (b), (c) and (d) present the regions around the (111), (001) and (002) peaks of CoPt. In these panels we used the square root of the intensity, in order to make the weak peaks more clearly visible.

having a Full Width at Half Maximum (FWHM) equal to 67 keV, solid angle 2.54 msr (steradian is the SI unit of solid angle with symbol sr) and total beam charge 32 μCb. The pressure in the goniometer chamber was 2×10^{-7} Torr.

Note: Despite the fact that the annealing process may (partially or fully) destroy the layer-by-layer structure of an as-deposited film, we will use the layer structure of the as-deposited film as a label for the post-annealed film. For instance, a multilayer with structure Si(001)/[Ag(0.5nm)/CoPt(4.5nm)]×4 before annealing will be named "post-annealed Si(001)/[Ag(0.5nm)/CoPt(4.5nm)]×4 NC" after the annealing process.

3. Experimental results and discussion

3.1. Crystallographic data of post-annealed plain CoPt films and Ag/CoPt BLs

For completeness reasons, we present here in short a comparison between the XRD data of post-annealed plain CoPt monolayers (MNLs) and the XRD data of post-annealed Ag/CoPt BLs. Representative X-ray data are shown in Fig. 1, where we present XRD spectra of a Si/Ag(1.2nm)/CoPt(48nm) BL before (as-deposited) and after annealing at 600^{o}C for 20 min (post-annealed). These values of annealing temperature and annealing time were chosen, because for annealing at lower temperatures or for shorter time periods the degree of $L1_0$-ordering and (001) texture were not satisfying. The XRD spectrum of a post-annealed Si/CoPt(48nm) MNL was added for comparison reasons. The as-deposited Ag/CoPt BL shows only a weak and broad

CoPt(111) peak, indicating that it is (111) textured and the CoPt grains are quite small. The absence of any other CoPt peaks shows that it contains only the disordered FCC phase of CoPt: the characteristic superstructure peaks of $L1_0$-CoPt [5, 51] are absent. The (111) texture is expected, because the (111) plane is the close-packed plane of FCC structure [28] with minimized surface energy. The subsequent annealing has as an effect not only the formation of the $L1_0$ phase of CoPt, but also typically leads to grain growth and sintering or coalescence [52, 53] which results in larger grains. Therefore, the post-annealed films should exhibit more intense and narrow peaks compared to the corresponding peaks of the as-deposited ones. The post-annealed Si/CoPt(48nm) MNL, which is a mixture of FCC-CoPt and $L1_0$-CoPt, does indeed show a strong and sharp CoPt(111) peak, but the other CoPt peaks are very weak. This MNL clearly shows a (111) texture, in agreement with Ref. [54] which reports that (in the case of FePt) the (111) plane has the lowest surface energy in both FCC and $L1_0$ structures. The fact that the (111), (001) and (002) peaks of CoPt are very weak in the post-annealed MNL indicates a relatively low degree of $L1_0$-ordering. The presence of $L1_0$-CoPt is mainly indicated by the fact that the CoPt(111) peak of the post-annealed MNL is placed at an angle 2θ relatively higher than the CoPt(111) peak of the as-deposited BL ($\Delta(2\theta)\approx 0.5^o$), as a result of the deformation of the unit cell during the FCC to $L1_0$ transformation.

In contrast to the behavior of the post-annealed MNL, the post-annealed BL shows a sufficient degree of $L1_0$-ordering, and a strong (001) texture. Indeed we observe strong and sharp CoPt(001) and CoPt(002) peaks and a clear CoPt(003) peak, while the CoPt(111) peak is weak. The presence of the CoPt(001) and CoPt(003) superstructure peaks is a clear evidence for the presence of the $L1_0$-phase of CoPt [5]. For the intensity ratio I_{001}/I_{002}, which is proportional to the square of the $L1_0$-ordering parameter [5, 13], we have $I_{001}/I_{002}\approx 1$. This shows a sufficient degree of $L1_0$-ordering, compared to the value 1.286 (see second paragraph of section 2). The development of the CoPt(00l) peaks, combined with the weak CoPt(111) peak, shows strong (001) texture. Using the measure I_{002}/I_{111} of the developed texture, we indeed see that $I_{002}/I_{111}\gg 1$. The absence of the CoPt(200) peak in the spectrum of the post-annealed BL is probably the result of the combination of the good $L1_0$-ordering with the strong (001) texture. We conclude that the presence of the Ag underlayer has as an effect the enhancement of $L1_0$-formation (and of the degree of $L1_0$-ordering) and simultaneously the development of (001) texture, compared to the (111) texture of the MNL.

3.2. HIRBS data on the post-annealed Ag/CoPt NCs

The annealing process at 600^oC, in order to achieve the formation of the $L1_0$ phase of CoPt, is expected to stimulate inter-diffusion between the two kinds of layer (CoPt magnetic layer, Ag layer) of the as-deposited film. The degree of this inter-diffusion was determined by HIRBS measurements on selected samples (mostly post-annealed Ag/CoPt NCs). Representative HIRBS data are shown in Fig. 2(a), where we present the HIRBS spectrum of a post-annealed Si/[Ag(0.5nm)/CoPt(4.5nm)]×4 NC (annealed at 600^oC for 40 min). Figures 2(b), 2(c) and 2(d) present the layer-by-layer structure after the annealing process, which was calculated by simulating the spectrum of Fig. 2(a) with the RUMP program: the simulation calculates the atomic stoichiometries of Ag, Pt and Co inside the NC film as functions of the distance from Si surface. The analysis of the spectrum showed that: (i) the film is continuous, (ii) there is indeed inter-diffusion between the Ag and CoPt layers during the annealing process. Although there is this inter-diffusion, the mixing between the two kinds of layers is not complete even for the elevated annealing temperature of 600^oC and the increased annealing time of 40 min. For this reason it is convenient to describe the structure of the post-annealed NC as a succession of "magnetic" (pure CoPt before annealing) and "spacer" (pure Ag before annealing) layers with thickness of 4.5 and 0.5 nm respectively, according to the as-deposited multilayer structure. The atomic stoichiometries $X_{\rm Ag}$, $X_{\rm Pt}$ and $X_{\rm Co}$ of Ag, Pt and Co respectively (as functions of the

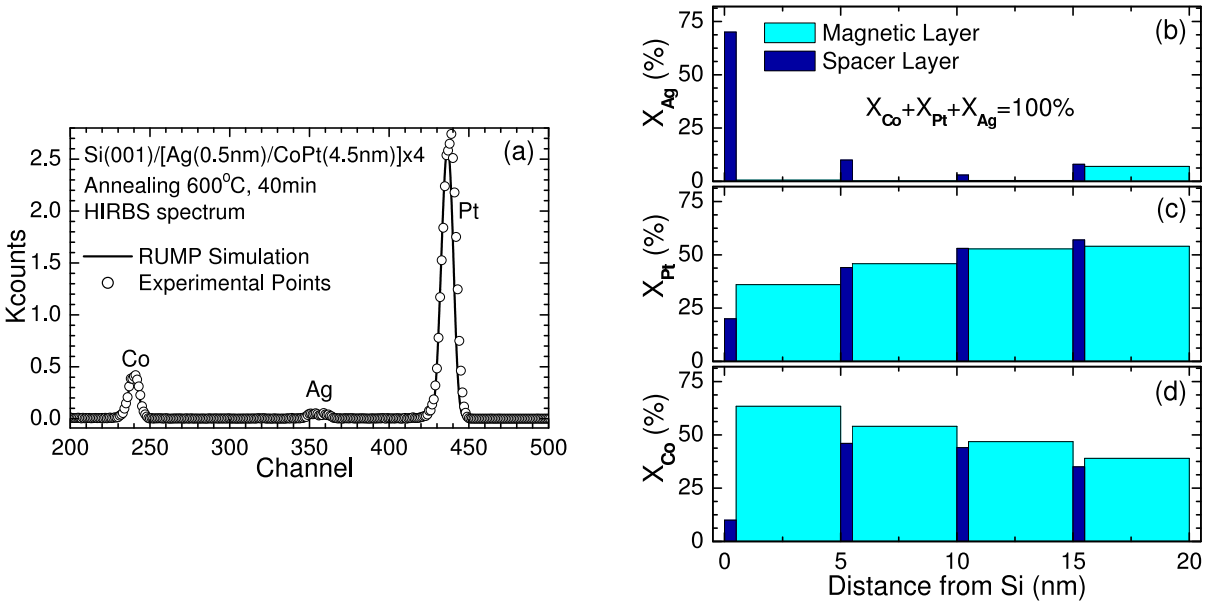

Figure 2. HIRBS spectrum (panel (a)) of a 20 nm thick Si(001)/[Ag(0.5nm)/CoPt(4.5nm)]×4 post-annealed NC. The continuous line is the result of the RUMP simulation that was used for the calculation of the chemical profile of the NC from the experimental points (open circles). Panels (b), (c) and (d) show the results of the calculation: the atomic stoichiometries $X_{\rm Ag}$, $X_{\rm Pt}$ and $X_{\rm Co}$ of Ag, Pt and Co respectively as functions of the distance from Si substrate. Dark (bright) bars correspond to film areas that were 100% occupied by Ag (CoPt) in the initial as-deposited multilayer.

distance from Si substrate) are shown in Figs. 2(b), 2(c) and 2(d) in histogram form: the dark (bright) bars represent the "spacer" ("magnetic") layers of the post-annealed film. In these figures we observe that:

(a) Inside the magnetic layers it is $X_{\rm Ag}\approx 0$, except from the magnetic layer at the top of the film. In the inner spacer layers, $X_{\rm Ag}$ also takes small – but not vanishing – values. We conclude that Ag shows a strong tendency to remain away from the magnetic layers and to move near the film-substrate interface and the top region of the NC film. In the case of BLs, where Ag exists in the as-deposited film only as an underlayer, Ag is expected to remain near the substrate during annealing. In the case of NCs, the small amount of Ag at the inner regions of the post-annealed film (the not vanishing $X_{\rm Ag}$ at the inner spacer layers) may result in the structural incoherence of the growth of the CoPt grains during annealing.

(b) Deviations from the equiatomic CoPt composition of the as-deposited film are observed, with the relative Co concentration $X_{\rm Co}$ increasing in layers next to the Si substrate. This gradient can be explained by Co-Si alloying at the substrate-film interface.

(c) Pt diffuses in Ag layers more easily than Co. Thus the Pt stoichiometry $X_{\rm Pt}$ varies smoothly with depth, while Co stoichiometry $X_{\rm Co}$ is reduced in spacer regions. This difference can be a result of the fact that Co is almost immiscible in Ag [4].

3.3. $L1_0$ formation and development of (001) texture in post-annealed Ag/CoPt BLs and NCs

In Ref. [25] we presented crystallographic data which showed the dependence of I_{001}/I_{002} ($L1_0$-ordering) and I_{002}/I_{111} (texture) from the thickness $t_{\rm CoPt}$ of the CoPt layer of post-annealed Ag/CoPt BLs. These data showed that the samples which exhibited the higher (lower) degree of (001) texture were also characterized by better (worse) $L1_0$-ordering, which suggested that there

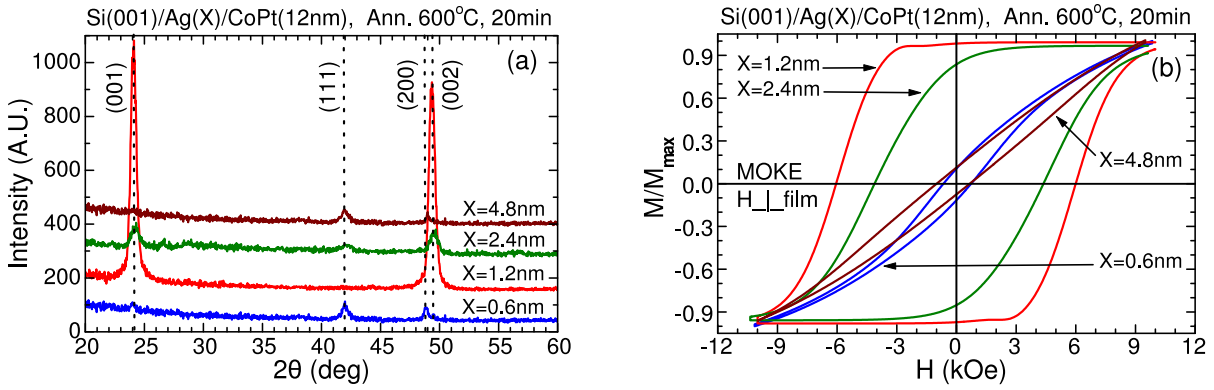

Figure 3. XRD spectra (panel (a)) and normalized MOKE hysteresis loops for $H\perp$film (panel (b)), of post-annealed Si(001)/Ag(X)/CoPt(12nm) BLs with X=0.6, 1.2, 2.4, 4.8 nm (annealing at 600^{o}C for 20 min).

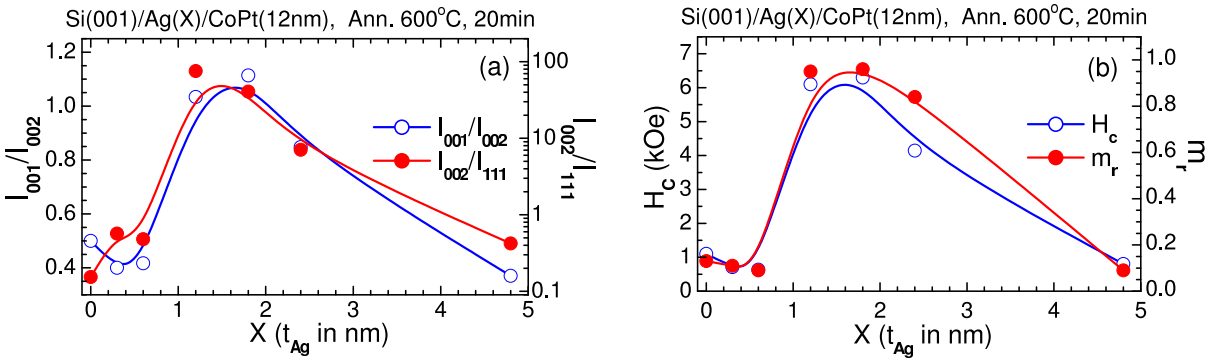

Figure 4. (a) L1$_0$-ordering (I_{001}/I_{002}, open circles) and crystallographic texture (I_{002}/I_{111}, solid circles), calculated from the XRD spectra of post-annealed Si(001)/Ag(X)/CoPt(12nm) BLs (600^{o}C for 20 min), presented as functions of X. (b) Coercivity H_c (open circles) and relative remnant magnetization m_r=M_r/M_s (solid circles), calculated from MOKE measurements on the same post-annealed BLs (for $H\perp$film), presented as functions of X. X (Ag layer thickness) takes the values X=0, 0.3, 0.6, 1.2, 1.8, 2.4, 4.8 nm.

is a correlation between the mechanisms of texture and ordering. We also presented the results of VSM (Vibrating Sample Magnetometer) measurements on post-anneled BLs with strong (001) texture, which showed that (001)-textured samples exhibit perpendicular magnetic anisotropy. This is an expected behavior, since the CoPt grains are highly aligned in a direction with the c-axis (easy axis) normal to the plane of the film and the L1$_0$ phase of CoPt is characterized by large uniaxial anisotropy. Here we present new XRD data concerning the dependence of ordering and texture from the thickness $t_{\rm Ag}$ of the Ag layer. These data, combined with the results of magnetization (MOKE) measurements, provide further evidence for the existence of the the above mentioned correlation. For the purposes of this study we prepared two series of BL samples with varying $t_{\rm Ag}$: a series with $t_{\rm CoPt}$=12 nm and a series with $t_{\rm CoPt}$=48 nm. Figure 3 presents characteristic XRD spectra and MOKE hysteresis loops, obtained from the measurements that were performed on the series of BL samples with $t_{\rm CoPt}$=12 nm. It is clear that strong (001) texture results in high coercivity and relative remnant magnetization for $H\perp$film.

The results extracted from all the XRD and MOKE measurements, performed on the series of BL samples with $t_{\rm CoPt}$=12 nm, are shown in Fig. 4: panel (a) presents I_{001}/I_{002} (L1$_0$-

ordering) and I_{002}/I_{111} (texture) as functions of t_{Ag}, panel (b) presents coercivity H_c and relative remnant magnetization m_r=M_r/M_s as functions of t_{Ag}. Both panels of Fig. 4 clearly show a correlation between ordering and texture and between H_c and m_r. The correlation of the magnetic quantities is probably a manifestation of the correlation between ordering and texture. Indeed, it is expected [10, 12] that higher degree of formation of the $L1_0$ phase of CoPt corresponds to higher coercivity H_c, as long as the sample is not fully ordered (CoPt has not been completely transformed into its $L1_0$ phase). Also it is expected that, for stronger (001) texture, the relative remnant magnetization in a direction normal to the film's plane will tend to increase. For stronger (001) texture, the alignment of the easy axis of magnetization (c-axis) of grains along a direction normal to the film's plane is enhanced. Therefore the remnant magnetization normal to film's plane is expected to increase, since for zero field is along the easy axis. Here the correlation between the mechanisms of texture and $L1_0$-ordering becomes more evident and it is clear that the Ag underlayer is strongly involved in this correlation, since its thickness variation causes a variation to the values of both I_{001}/I_{002}-H_c and I_{002}/I_{111}-m_r.

From the HIRBS data, which were presented in subsection 3.2, we know that the Ag underlayers of the as-deposited BLs tend to remain at the film-Si(001) interface after the annealing process. This is a strong indication that the mechanism, through which Ag influences both ordering and texture, is of interfacial origin. However this does not indicate which is the nature of this mechanism, and does not explain the dependence of ordering and texture on t_{Ag}. In order to be able to make assumptions on the nature of this mechanism, we need a description of the Ag-Si(001) system. According to Refs. [55, 56, 57, 58, 59, 60, 61], this system exhibits the following properties:

(a) Although the Ag-Si(001) system exhibits high lattice mismatch [a_{Si}=5.431 Å (diamond), a_{Ag}=4.086 Å (FCC)], the ratio of Si to Ag lattice constants is almost exactly equal to 4:3. Therefore the two lattices can be adjusted with a very small remaining mismatch (2.2%).

(b) The Stranski-Krastanov (SK) mode of growth [62, 63] for Ag is well established. At the early stages of growth, Ag grows in 2D islands. In these 2D islands, the orientation relationship between Ag and Si is $(001)_{Ag}\|(001)_{Si}$ and Ag shows (001) texture. It continues to form a 2D Ag layer until Si coverage takes a critical value at about 0.5 ML, or equivalently at 2 nm [63, 64]. Above this value, the growth mode becomes gradually 3D. For 1 ML Ag forms 3D islands. The $\langle 111\rangle$ becomes gradually the preferred growth orientation and Ag shows (111) texture, due to the lowest surface free energy for the (111) surface of the FCC crystals. This behavior is valid even at elevated temperatures (possibly with different critical value of thickness).

(c) With the sputtering process we can produce almost "epitaxial" Ag grains with (001) texture, in the initial stage of Ag growth, at a low sputtering power.

The proposed mechanism, for the explanation of the correlation between ordering and (001) texture development, is based on the reduction of total microstrain through the annealing process and is in good agreement (at least qualitatively) with the experimental data. Microstrain minimization in similar Ag/CoPt NCs has already been observed in Refs. [33, 34] (using XRD-peak profile analysis) and has been correlated to the optimization of (001) texture. In Ref. [28] Yu-Nu Hsu et al reported that the presence of (001) textured Ag underlayer is possible to induce (001) texturing in epitaxial FePt films and reduce the annealing temperature that is necessary for $L1_0$-formation. Since the Ag lattice parameter (a_{Ag}=4.086 Å) is slightly larger than that of FePt [65] (as also of CoPt [51]), the epitaxial growth is achieved via distortion of FePt (or Copt) unit cell and expansion of the unit cell constants along the film-Ag interface. On the other hand, during the cubic to tetragonal transformation (throughout the annealing process), the a and b axes expand while the c-axis contracts. This creates a mechanism by which the (001) texturing and ordering processes are correlated and the microstrain of FePt or CoPt is reduced, as a result of the reduction of the lattice mismatch with Ag. Also the surface energy must be minimized. In Ref. [54] Jae-Song Kim *et al* also studied the origin of (001) texture of FePt films.

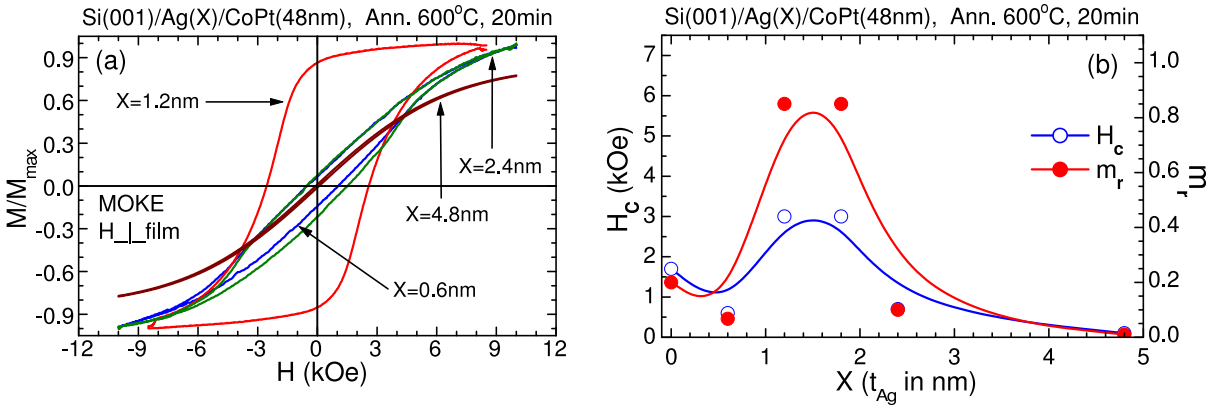

Figure 5. (a) Normalized MOKE hysteresis loops for $H\perp$film, of post-annealed Si(001)/Ag(X)/CoPt(48nm) BLs with X=0.6, 1.2, 2.4, 4.8 nm (annealing at 600^{o}C for 20 min). (b) Coercivity H_c (open circles) and relative remnant magnetization m_r=M_r/M_s (solid circles), presented as functions of X. H_c and m_r were calculated from the MOKE measurements presented in panel (a) (only the most representative loops are shown there). X (Ag layer thickness) takes the values X=0, 0.6, 1.2, 1.8, 2.4, 4.8 nm.

They distinguished the terms that contribute in the total energy of the polycrystalline material in three categories: (a) surface energy anisotropy [66], since surface energy depends on Miller indices (hkl), (b) biaxial in-plane strain caused by various sources such as residual strain of as-deposited film [66], difference in the thermal expansion coefficient between film and substate [67] (or in our case also between underlayer and top layer) and volume shrinkage in films by defect elimination and grain growth [68] during annealing, (c) anisotropic transormation strain due to the deformation of the unit cell during FCC to $L1_0$ transformation throughout annealing. According to Ref. [54], the formation of the (001) texture during annealing results from the minimization of the total energy, in which the 3rd term is the dominant term.

The above described mechanism, combined with the behavior of the Ag-Si(001) system can explain our experimental data. In Fig. 4 the region for Ag thickness lower than 1.2 nm should correspond to the first stage of Ag growth on Si(001), i.e. 2D almost "epitaxial" with (001) texture. The coverage of Si with Ag increases with $t_{\rm Ag}$. As a result, larger regions of the CoPt layer are influenced by the described mechanism and the ordering and texture are increased with $t_{\rm Ag}$. The region for $t_{\rm Ag}$>2 nm should correspond to the stage where Ag growth becomes gradually 3D with (111) texture, and the mechanism becomes weaker with the increment of $t_{\rm Ag}$. The coherence of growth of (001) textured CoPt is disrupted by the Ag island growth with (111) texture. The optimum Ag underlayer thickness is in the region 1.2–2 nm. Also the strain relaxation along film thickness can be more effectively realized in very thin films, through the formation of islands. This may be the reason for the relatively lower coercivity H_c and relative remnant magnetization m_r values of Fig. 5 when compared to the values of Fig. 4. Figure 5 presents the MOKE measurements performed on the series of BL samples with $t_{\rm CoPt}$=48 nm. For this series of samples, the optimum Ag underlayer thickness is also in the region 1.2–2 nm.

In subsection 3.2, where we studied the HIRBS data of post-annealed NCs, we concluded that the small amount of Ag at the inner regions of a post-annealed Ag/CoPt NC (the not vanishing atomic percentage of Ag at the inner spacer layers) may result in the structural incoherence of the growth of the CoPt grains during annealing. Figure 6 shows crystallographic data that support this conclusion. Panel (a) shows texture and ordering as functions of the thickness of the CoPt layer for BLs with 1.2 nm of Ag underlayer. Correlation between texture and ordering is evident. Panel (b) shows texture as function of the total thickness for NCs with 10% Ag,

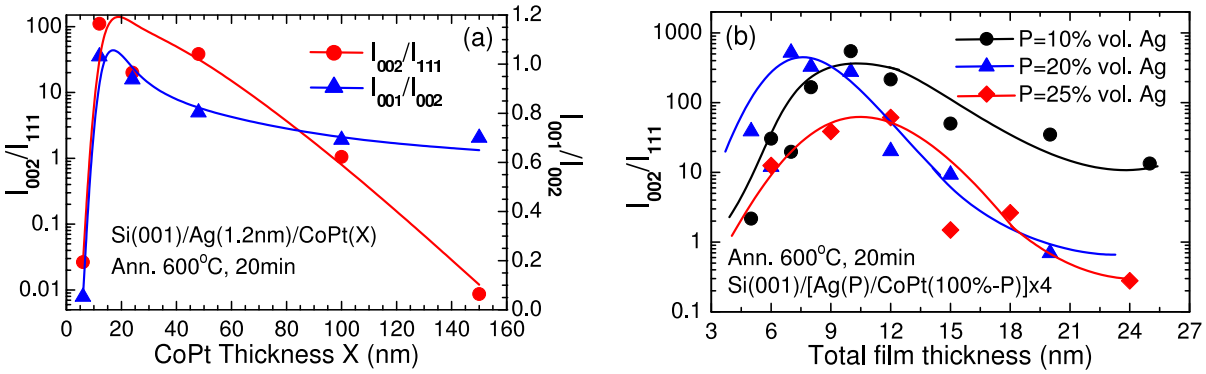

Figure 6. Comparison between the textures developed on post-annealed BLs and NCs. Panel (a) shows texture (circles) and ordering (triangles) as functions of the thickness of the CoPt layer for BLs with 1.2 nm of Ag underlayer. Panel (b) shows texture as function of the total thickness for NCs with 10% Ag (circles), 20% Ag (triangles) and 25% Ag (rhombs). Percentage refers to volume.

20% Ag and 25% Ag. Percentage refers to volume. First we observe that increment of the percentage of Ag results gradually in an overall reduction of the texture developed in the NC, which is compatible with the hypothesis of structural incoherence due to the presence of Ag in the inner regions of the film. Direct comparison of the degree of (001) texture between BLs and NCs, shows that in the case of NCs the (001) texture starts to degrade for lower total film thickness compared to the case of BLs. For NCs with total film thickness near 9–12 nm it is $I_{002}/I_{111}\approx500$, compared to the value $I_{002}/I_{111}\approx100$ exhibited by the BLs. In contrast to that, for NCs with total thickness above 15 nm, the degree of (001) texture is already lower than the value $I_{002}/I_{111}\approx40$, while for BLs it is $I_{002}/I_{111}\approx50$ even for 50 nm total thickness. This is also compatible with the hypothesis of structural incoherence.

3.4. Conclusions

The basic conclusions that can be deduced from the X-ray, magnetization and HIRBS data presented in this work, for post-annealed Ag/CoPt BLs and NCs, are the following:

- Ag underlayers can promote a high degree of $L1_0$-ordering and a strong (001) crystallographic texture in the post-annealed Ag/CoPt BLs. CoPt films without Ag underlayers have a (111) texture.
- The influence of Ag underlayers on post-annealed Ag/CoPt BLs is Ag and CoPt thickness dependent, as it is shown by both magnetic and XRD measurements. It was found that the optimum thickness of the Ag underlayer, for the development of strong (001) crystallographic texture in the post-annealed BLs, is $t_{Ag}\approx1.2$–2.0 nm. For Ag thickness within this range of values, the post-annealed BLs develop a strong (001) texture. For values of t_{Ag} outside this range, the post-annealed BLs tend to develop a (111) texture (this includes the CoPt MNLs, which correspond to $t_{Ag}=0$ nm).
- It was also found that the degree of (001) crystallographic texture (represented by I_{002}/I_{111}) and the degree of $L1_0$-ordering (represented by I_{001}/I_{002}), of the post-annealed BLs, are correlated. Indeed, XRD measurements for various values of t_{Ag} showed that: the maximum (medium or minimum) values of I_{002}/I_{111} correspond to maximum (medium or minimum) values of I_{001}/I_{002}. This correlation was also observed in the magnetic measurements.
- The HIRBS data of post annealed Ag/CoPt NCs show a very strong tendency of Ag to remain near film-substrate interface, as well as at the top region of the film, after the

annealing process. Especially in the case of BLs, Ag underlayers tend to remain near the Ag-Si(001) interface. This suggests that the mechanism responsible for the correlation between $L1_0$-formation and development of (001) texture is of interfacial origin.

- The mechanism, that is proposed for the explanation of this correlation, is based on the reduction of total strain (residual strain of as-deposited film and transformation strain due to deformation of the unit cell as $L1_0$-CoPt is formed) throughout the annealing process and the accompanied reduction of the lattice mismatch with the Ag underlayer.
- Comparison of the degree of (001) crystallographic texture between BLs and NCs, shows that in the case of NCs the (001) texture starts to degrade for lower total film thickness compared to the case of BLs. For NCs with total film thickness near 9–12 nm it is $I_{002}/I_{111}\approx500$, compared to the value $I_{002}/I_{111}\approx100$ exhibited by the BLs. In contrast to that, for NCs with total thickness above 15 nm, the degree of (001) texture is already lower than the value $I_{002}/I_{111}\approx40$, while for BLs it is $I_{002}/I_{111}\approx50$ even for 50 nm total thickness. This difference can be explained by the structural incoherence in the growth of the CoPt grains, imposed by the presence of intermediate spacer layers (which contain Ag) during the annealing process.

References

[1] Cullity B D 1972 *Introduction to Magnetic Materials* (Addison-Wesley Publishing Company)
[2] O'Handley R C 2000 *Modern Magnetic Materials: Principles and Applications* (John Wiley & Sons Inc.)
[3] Barrett C S and Massalski T B 1966 *Structure of Metals* (New York: McGraw-Hill)
[4] Massalski T B 1996 *Binary Alloy Phase Diagrams* (ASM International)
[5] Warren B E 1990 *X-ray Diffraction* (New York: Dover)
[6] Darling A S 1963 *Platinum Met. Rev.* **7** 96
[7] McCurrie R A and Gaunt P 1966 *Philos. Mag.* **13** 567
[8] Gaunt P 1966 *Philos. Mag.* **13** 579
[9] Brissonneau P, Blanchard A, Schlenker M and Laugier J 1968 *J. Appl. Phys.* **39** 1266
[10] Yermakov A Y and Maykov V V 1985 *Fiz. Met. Metalloved.* **60** 113
[11] Klemmer T, Hoydick D, Okumura H, Zhang B and Soffa W A 1995 *Scr. Metall. Mater.* **33** 1793
[12] Ristau R A, Barmak K, Lewis L H, Coffey K R and Howard J K 1999 *J. Appl. Phys.* **86** 4527
[13] Barmak K, Kim J, Lewis L H, Coffey K R, Toney M F, Kellock A J and Thiele J-U 2005 *J. Appl. Phys.* **98** 033904
[14] Coffey K R, Parker M A and Howard J K 1995 *IEEE Trans. Magn.* **31** 2737
[15] Yanagisawa M, Shiota N, Yamaguchi H and Suganuma Y 1983 *IEEE Trans. Magn.* **19** 1638
[16] Weller D and Moser A 1999 *IEEE Trans. Magn.* **35** 4423
[17] Weller D, Moser A, Folks L, Best M E, Lee W, Toney M F, Schwickert M, Thiele J-U and Doerner M F 2000 *IEEE Trans. Magn.* **36** 10
[18] Wang J-P, Qiu J-M, Taton T A and Kim B-S 2006 *IEEE Trans. Magn.* **42** 3042
[19] Jones B A, Dutson J D, OGrady K, Hickey B J, Li D, Poudyal N and Liu J P 2006 *IEEE Trans. Magn.* **42** 3066
[20] Sun A-C, Hsu J-H, Kuo P C and Huang H L 2007 *IEEE Trans. Magn.* **43** 2130
[21] Luo C P and Sellmyer D J 1995 *IEEE Trans. Magn.* **31** 2764
[22] Luo P, Shan Z S and Sellmyer D J 1996 *J. Appl. Phys.* **79** 4899
[23] Farrow R F C, Weller D, Marks R F, Toney M F, Cebollada A and Harp G R 1996 *J. Appl. Phys.* **79** 5967
[24] Liao W M, Lin Y P, Yuan F T and Chen S K, 2004 *J. Magn. Magn. Mater.* **272–276** 2175
[25] Manios E, Karanasos V, Niarchos D and Panagiotopoulos I 2004 *J. Magn. Magn. Mater.* **272–276** 2169
[26] Manios E, Alexandrakis V and Niarchos D 2007 *J. Magn. Magn. Mater.* **316** E166
[27] Hsu Y-N, Jeong S, Laughlin D E and Lambeth D N 2001 *J. Appl. Phys.* **89** 7068
[28] Hsu Y-N, Jeong S, Laughlin D E and Lambeth D N 2003 *J. Magn. Magn. Mater.* **260** 282
[29] Yu M, Liu Y and Sellmyer D J 1999 *Appl. Phys. Lett.* **75** 3992
[30] Luo C P, Liou S H, Gao L, Liu Y and Sellmyer D J 2000 *Appl. Phys. Lett.* **77** 2225
[31] Karanasos V, Panagiotopoulos I, Niarchos D, Okumura H and Hadjipanayis G C 2000 *J. Appl. Phys.* **88** 2740
[32] Karanasos V, Panagiotopoulos I, Niarchos D, Okumura H and Hadjipanayis G C 2001 *J. Appl. Phys.* **90** 3112

[33] Karanasos V, Panagiotopoulos I, Niarchos D, Okumura H and Hadjipanayis G C 2001 *Appl. Phys. Lett.* **79** 1255
[34] Karanasos V, Panagiotopoulos I and Niarchos D 2002 *J. Magn. Magn. Mater.* **249** 471
[35] Christodoulides J A, Bonder M J, Huang Y, Zhang Y, Stoyanov S, Hadjipanayis G C, Simopoulos A and Weller D 2003 *Phys. Rev. B* **68** 054428
[36] Tomou A, Panagiotopoulos I, Gournis D and Kooi B 2007 *J. Appl. Phys.* **102** 023910
[37] Plumer M L, van Ek J and Weller D (Editors) 2001 *The Physics of Ultra-High-Density Magnetic Recording* (Springer - Springer Series in Surface Sciences)
[38] Zeng H, Yan M L, Powers N and Sellmyer D J 2002 *Appl. Phys. Lett.* **80** 2350
[39] Luo C P and Sellmyer D J 1999 *Appl. Phys. Lett.* **75** 3162
[40] Sellmyer D J, Luo C P, Yan M L and Liu Y 2001 *IEEE Trans. Magn.* **37** 1286
[41] Yan M L, Zeng H, Powers N and Sellmyer D J 2002 *J. Appl. Phys.* **91** 8471
[42] Yan M L, Powers N and Sellmyer D J 2003 *J. Appl. Phys.* **93** 8292
[43] Yan M L, Li X Z, Gao L, Liou S H and Sellmyer D J 2003 *Appl. Phys. Lett.* **83** 3332
[44] Shao Y, Yan M L and Sellmyer D J 2003 *J. Appl. Phys.* **93** 8152
[45] Yan M L, Sabirianov R F, Xu Y F, Li X Z and Sellmyer D J 2004 *IEEE Trans. Magn.* **40** 2470
[46] Sellmyer D J, Yan M, Xu Y and R. Skomski R 2005 *IEEE Trans. Magn.* **41** 560
[47] Chen J S, Lim B C, Hu J F, Liu B, Chow G M and Ju G 2007 *Appl. Phys. Lett.* **91** 132506
[48] Wu Y-C, Wang L-W and Lai C-H 2007 *Appl. Phys. Lett.* **91** 072502
[49] Li B-H, Feng C, Gao X, Teng J, Yu G-H, Xing X and Liu Z-Y 2007 *Appl. Phys. Lett.* **91** 152502
[50] Yang F J, Wang H, Wang H B, Cao X, Yang C P, Li Q, Zhou M J, Chong Y M and Zhang W J 2007 *J. Appl. Phys.* **102** 106101
[51] $L1_0$-CoPt: JCPDS-ICDD database, card No 43-1358; Axes lengths of $L1_0$-CoPt unit cell: $a = 3.803$ Å and $c = 3.701$ Å.
[52] Dai Z R, Sun S and Wang Z L 2001 *Nano Lett.* **1** (8) 443
[53] Klemmer T J, Liu C, Shukla N, Wu X W, Weller D, Tanase M, Laughlin D E and Soffa W A 2003 *J. Magn. Magn. Mater.* **266** 79
[54] Kim J-S, Koo Y-M, Lee B-J and Lee S-R 2006 *J. Appl. Phys.* **99** 053906
[55] Lin X F, Wan K J and Nogami J 1993 *Phys. Rev. B* **47** 13491
[56] Lin X F, Wan K J and Nogami J 1994 *Phys. Rev. B* **49** 7385
[57] Doraiswamy N, Jayaram G and Marks L D 1995 *Phys. Rev. B* **51** 10167
[58] Kimura K, Ohshima K and Mannami M 1995 *Phys. Rev. B* **52** 5737
[59] von Hoegen M H, Schmidt T, Meyer G, Winau D and Rieder K H 1995 *Phys. Rev. B* **52** 10764
[60] Glueckstein J C, Evans M M R and Nogami J 1996 *Phys. Rev. B* **54** R11066
[61] Je J H, Kang T S and Noh D Y 1997 *J. Appl. Phys.* **81** 6716
[62] Zangwill A 1988 *Physics at Surfaces* (Cambridge University Press).
[63] Venables J A 2001 *Introduction to Surface and Thin Film Processes* (Cambridge University Press).
[64] The monolayer (ML) unit is a measure of areal density of atoms and it is expressed as atoms/m^2. 1ML corresponds to the areal density of one monolayer of atoms.
[65] FCC-FePt: JCPDS-ICDD database, card No 29-0717 and 29-0718; $L1_0$-FePt: JCPDS-ICDD database, card No 43-1359; Axes lengths of $L1_0$-FePt unit cell: $a = 3.852$ Å and $c = 3.713$ Å.
[66] Thompson C V and Carel R 1995 *Mater. Sci. Eng.* **B-32** 211
[67] Witt F and Vook R W 1968 *J. Appl. Phys.* **39** 2773
[68] Zeigera W, Brucknerb W, Schumannb J, Pitschkeb W and Worcha H 2000 *Thin Solid Films* **370** 315